



# **A Comparison between a Model-free and Model-based Controller of an Automotive Semi-active Suspension System : Independent Wheel-stations**

Juan C. Tudon-Martinez, Rubén Morales-Menéndez, Ricardo A. Ramirez-Mendoza,  
Olivier Sename, Luc Dugard

## **► To cite this version:**

Juan C. Tudon-Martinez, Rubén Morales-Menéndez, Ricardo A. Ramirez-Mendoza, Olivier Sename, Luc Dugard. A Comparison between a Model-free and Model-based Controller of an Automotive Semi-active Suspension System : Independent Wheel-stations. IFAC Joint conference SSSC - 5th Symposium on System Structure and Control, Feb 2013, Grenoble, France. pp.869-874, <10.3182/20130204-3-FR-2033.00039>. <hal-00817534>

**HAL Id: hal-00817534**

**<https://hal.science/hal-00817534v1>**

Submitted on 24 Apr 2013

**HAL** is a multi-disciplinary open access archive for the deposit and dissemination of scientific research documents, whether they are published or not. The documents may come from teaching and research institutions in France or abroad, or from public or private research centers.

L'archive ouverte pluridisciplinaire **HAL**, est destinée au dépôt et à la diffusion de documents scientifiques de niveau recherche, publiés ou non, émanant des établissements d'enseignement et de recherche français ou étrangers, des laboratoires publics ou privés.



HAL Authorization

# Comparison between a Model-free and Model-based Controller of an Automotive Semi-active Suspension System: Independent Wheel-stations <sup>★</sup>

Juan C. Tudón-Martínez <sup>\*</sup> Ruben Morales-Menendez <sup>\*</sup>  
Ricardo Ramírez-Mendoza <sup>\*</sup> Olivier Sename <sup>\*\*</sup> Luc Dugard <sup>\*\*</sup>

<sup>\*</sup> *Tecnológico de Monterrey, Av. E. Garza Sada 2501, 64849, Monterrey N.L., México (e-mail: {jc.tudon.phd.mty, rmm, ricardo.ramirez}@itesm.mx)*

<sup>\*\*</sup> *GIPSA-lab, Control Systems Dept. CNRS-Grenoble INP, ENSE3, BP 46, F-38402 St Martin d'Hres cedex, France (e-mail: {olivier.sename, luc.dugard}@gipsa-lab.grenoble-inp.fr)*

---

**Abstract:** A comparison between two control strategies of automotive semi-active suspension systems is presented by using a pick-up truck model in CarSim<sup>TM</sup>; the controllers are based on different frameworks. The Linear Parameter Varying (LPV) controller, considered as model-based controller, includes the constraints of the semi-active damper by using two scheduling parameters; while, the Frequency Estimation-Based (FEB) controller only requires measurements of a wheel-station for defining the damping force according to the objective controls, i.e. is free of a vehicle and actuator model. Since each wheel-station has an independent controller, the global semi-active suspension control system does not include the coupling effect among the four vehicle corners; however this effect is embedded into the controller performance. Experimental data are used to model a MR damper, which is used in each quarter of vehicle. A bounce sine sweep test is used to compare the performance in comfort and road holding of both controllers. Simulation results in CarSim<sup>TM</sup> shows that the FEB controller has the best comfort and road holding performance; in comparison with the passive suspension system, the pitch angle is reduced 19%, the front and rear suspension deflection decrease 23% and 58% respectively and the tire compression is reduced 3% (front wheel) and 10% (rear wheel).

**Keywords:** Semi-active Suspension Control, Magneto-Rheological Damper, Linear Parameter Varying Control, Heuristic Control.

---

## 1. INTRODUCTION

Recently, suspension systems play a key role in vehicle design. In the standard ISO 2631, it has been established that the human body could suffer different health damages if this is exposed to constant vibrations, specially at frequencies between 0.5 - 20 Hz. Thus, the design in automotive suspension systems is focused to ensure not only the wheel-road contact (road holding) but also to improve the passengers comfort by isolating the road irregularities of the vehicle body. In contrast with passive suspension systems, which are designed mechanically and have constant damping ratio, the semi-active and active suspension systems can regulate the vehicle motions by using a control strategy over the damping force.

By good performance, low price, low energy consumption and easy implementation, the semi-active suspension systems are widely used in automobile industry nowadays. Commercially, there are different technologies of semi-active dampers, the main advantages of a

Magneto-Rheological (MR) damper versus others semi-active dampers are: (a) fast time response (20-40 ms), (b) large force range and, (c) long bandwidth of control.

An MR damper contains metallic particles into the oil that modify the rheological properties of the fluid when a magnetic field is manipulated by an electric current signal; the flow resistance variation causes a highly nonlinear behavior in the damping ratio. The MR damper in an Automotive Suspension Control System (ASCS) is used to dissipate the energy for reducing the motion in the sprung mass and maintaining the wheel-road contact.

The semi-active suspension control design has been tackled with many approaches based on different frameworks during last decades. For its facility of design and widely experimental evaluation, the classical Sky-Hook (SH) controller proposed by Karnopp et al. (1974) and its improvements such as the modified SH [Hong et al. (2002)], mixed SH-ADD [Savaresi and Spelta (2007)], *Mix-1-sensor* [Spelta et al. (2010)] and others, offer a good alternative to improve comfort; however, such control strategies neglect the road holding objective into the control law. In Sung et al. (2008), Sankaranarayanan et al. (2008) and Tudón-

---

<sup>★</sup> Authors thank to Tecnológico de Monterrey (Autotronics research chair) and CONACyT (PCP 03/2010) for their partial support.

Martínez et al. (2012) is showed the performance of some of these controllers by using a full vehicle semi-active suspension system with independent wheel-stations.

On the contrary, the Ground-Hook (*GH*) controller [Valasek et al. (1997)], designed in a similar way to *SH*, improves only the road holding. By combining the *SH* and *GH* techniques, the hybrid controller proposed in Ahmadian (1997) allows to improve both control objectives; however, a comparison between the hybrid controller and an heuristic control strategy, named *Frequency Estimation-Based (FEB)* controller proposed by Lozoya-Santos et al. (2011), shows that the heuristic approach has better results of comfort and handling in a full vehicle semi-active suspension system with softer changes in the manipulation of the semi-active dampers. Other heuristic controllers [Ikenaga et al. (2000), Swevers et al. (2007), Dong et al. (2009)], considered as free of model, have been designed to improve comfort in a vehicle, but they use a master controller to include the coupling features among the four wheel-stations and have been analyzed for small or medium-size vehicles and not pick-up trucks.

On the other hand, the nonlinear control techniques such as Linear Parameter-Varying (*LPV*) control [Poussot-Vassal et al. (2008), Do et al. (2010)] and Sliding Mode Control (*SMC*) [Assadsangabi et al. (2009)] offer interesting simulating results in a Quarter of Vehicle (*QoV*) design, where the objectives of comfort and road holding are considered into the control law by including the properties of hysteresis, saturation and semi-activity of the damper, e.g. the *LPV* approach presented in Do et al. (2010). These nonlinear techniques also are evaluated in full-vehicle models [Chamseddine et al. (2006), Yoon et al. (2010), Poussot-Vassal et al. (2011)] with good results; however, their design is considerable complex since two levels of control are demanded or different control modes are defined.

In this manner, by their good results in a *QoV* model, a comparative analysis between an *LPV* controller (model-based approach) and the *FEB* controller (model-free approach) is presented in this paper by using a full semi-active suspension system of a pick-up with independent controllers in the wheel-stations. In Lozoya-Santos et al. (2011) is presented a comparison between these controllers, but the analysis of performance does not include the nonlinear dynamics of a full-vehicle model and the *QoV* parameters correspond to a medium-size car. In Dong et al. (2010), a comparative research in semi-active control strategies for an *MR* suspension is presented, a nonlinear controller (*SMC*) showed the best performance in comfort but an heuristic controller (fuzzy) had the best road holding; the analysis is also based on a *QoV* system. Similarly, a quarter car test rig is used in Hudha et al. (2005) to compare the *SH*, *GH* and hybrid controller.

Based on robust control theory, the *LPV* controller is synthesized to improve comfort and road holding by using two scheduling parameters that include the constraints of the *MR* damper; thus, several experiments over a commercial *MR* damper are considered to model the nonlinearities of the semi-active damper dynamics. On the other hand, the *FEB* controller defines the electric current value to apply on the *MR* damper by bandwidths

according to the desired objective control (comfort or road holding) and using an estimated frequency signal of motion in the suspension. Physical insights of the vehicle are used to model it in CarSim<sup>TM</sup>, which is used as Software-in-the-Loop (*SiL*). The Bounce Sine Sweep (*BSS*) test is used to quantify the comfort and road holding performances in both controllers; the Root Mean Square RMS value over the variables of interest is used as performance index.

The outline of this paper is as follows: the formulation of the *LPV* controller is described in the next section. Section 3 presents the *FEB* controller design. Section 4 shows the simulation tests and a discussion of results is presented in 5. Finally, conclusions are presented in section 6.

Table 1. Definition of Variables.

| Variable        | Description                                             |
|-----------------|---------------------------------------------------------|
| $a_i$           | Pre-yield viscous damping coefficients                  |
| $b_i$           | Post-yield viscous damping coefficients                 |
| $f_c$           | Dynamic yield <i>MR</i> force                           |
| $F_{MR}$        | <i>MR</i> damping force                                 |
| $I$             | Electric current                                        |
| $k_s$           | Spring stiffness coefficient                            |
| $k_t$           | Stiffness coefficient of the wheel tire                 |
| $m_s$           | Sprung mass in the <i>QoV</i>                           |
| $m_{us}$        | Unsprung mass in the <i>QoV</i>                         |
| $u_{sat}$       | Filtered and bounded controller output                  |
| $\dot{z}_{def}$ | Damper piston velocity (deflection velocity)            |
| $z_r$           | Road profile (input disturbance)                        |
| $z_s$           | Vertical position of the mass $m_s$                     |
| $\dot{z}_s$     | Vertical velocity of the mass $m_s$                     |
| $\ddot{z}_s$    | Vertical acceleration of the mass $m_s$                 |
| $z_{us}$        | Vertical position of the mass $m_{us}$                  |
| $\dot{z}_{us}$  | Vertical velocity of the mass $m_{us}$                  |
| $\ddot{z}_{us}$ | Vertical acceleration of the mass $m_{us}$              |
| $\rho_1^*$      | Varying parameter for hysteresis/saturation of $F_{MR}$ |
| $\rho_2^*$      | Varying parameter for dissipativity constraint of $u$   |

## 2. LPV FORMULATION

In *LPV* controller design, first it is described the nonlinear behavior of the *QoV* system and then the gain scheduling parameters, used to achieve an *LPV* model, are defined.

### 2.1 QoV representation

An experimental *MR* damper model represents the suspension between both masses, Fig. 1. It is assumed that the wheel-road contact is ensured. All variables are described in Table 1. The system dynamics is given by:

$$\begin{aligned} m_s \ddot{z}_s &= -k_s(z_s - z_{us}) - F_{MR} \\ m_{us} \ddot{z}_{us} &= k_s(z_s - z_{us}) - k_t(z_{us} - z_r) + F_{MR} \end{aligned} \quad (1)$$

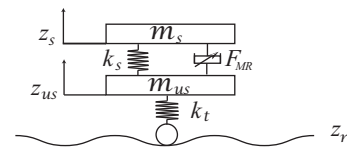


Fig. 1. Model for a *QoV* with a semi-active damper.

The *MR* damper model embedded in the *QoV* is represented by the parametric model of Guo et al. (2006), which emphasizes the hysteresis dependence on the position and

velocity of the piston by using a  $\tanh$  function. The characteristic of a linear elastomer is included, by representing a stiffness factor. The non-linear model is defined by:

$$F_{MR} = f_c \cdot \tanh(a_1 \dot{z}_{def} + a_2 z_{def}) + b_1 \cdot \dot{z}_{def} + b_2 \cdot z_{def} \quad (2)$$

where, the 5 coefficients have physical meaning, Table 1.

## 2.2 LPV modelling

Based on the *LPV* control framework proposed by Do et al. (2010), the varying parameter  $\rho_1$  is defined by the nonlinear term of the *MR* damping force of (2), such that:

$$\rho_1 = \tanh(a_1 \dot{z}_{def} + a_2 z_{def}) \in [-1, 1] \quad (3)$$

A general state-space representation of the *QoV* model can be obtained, rewriting (1), (2) and (3) as:

$$\begin{aligned} \dot{x}_s &= A_s \cdot x_s + B_s \cdot u + B_{s1} \cdot z_r \\ y &= C_s \cdot x_s \end{aligned} \quad (4)$$

where,  $u$  is the control input in N and,

$$\begin{aligned} y &= z_{def} = z_s - z_{us}, \quad C_s = [1 \ 0 \ -1 \ 0] \\ B_s &= \begin{bmatrix} 0 \\ -\rho_1 \\ m_s \\ 0 \\ \rho_1 \\ m_{us} \end{bmatrix}, \quad B_{s1} = \begin{bmatrix} 0 \\ 0 \\ 0 \\ k_t \\ m_{us} \end{bmatrix}, \quad x_s = \begin{bmatrix} z_s \\ \dot{z}_s \\ z_{us} \\ \dot{z}_{us} \end{bmatrix} \\ A_s &= \begin{bmatrix} 0 & 1 & 0 & 0 \\ -\frac{k_s + b_2}{m_s} & -\frac{b_1}{m_s} & \frac{k_s + b_2}{m_s} & \frac{b_1}{m_s} \\ 0 & 0 & 0 & 1 \\ \frac{k_s + b_2}{m_{us}} & \frac{b_1}{m_{us}} & -\frac{k_s + b_2 + k_t}{m_{us}} & -\frac{b_1}{m_{us}} \end{bmatrix}, \quad u = f_c \end{aligned}$$

In order to satisfy the dissipativity constraint in the control input, the state-space representation of (4) is rewritten in (5) and  $u = f_c - f_0$ , details in Do et al. (2010).

$$\begin{aligned} \dot{x}_s &= (A_s + B_{s2} \cdot \rho_2 \cdot C_{s2}) \cdot x_s + B_s \cdot u + B_{s1} \cdot z_r \\ y &= C_s \cdot x_s \end{aligned} \quad (5)$$

$$B_{s2} = \begin{bmatrix} 0 & -\frac{f_0}{m_s} & 0 & \frac{f_0}{m_s} \end{bmatrix}^T, \quad C_{s2} = [a_2 \ a_1 \ -a_2 \ -a_1]$$

where,  $f_0$  is the average of  $f_c$  and  $\rho_2 = \frac{\rho_1}{C_{s2} x_s} \in [0, 1]$ .

Since the controlled input matrix  $B_s$  depends on  $\rho_1$ , it is required to add a low pass filter into de *QoV* model for getting a proper structure for the *LPV* based controller synthesis, Poussot-Vassal et al. (2008). Additionally, a saturation constraint ( $\rho_{sat}$ ) is embedded into the filter for does not affect the closed-loop behavior.

A filter with bandwidth of 25 Hz was used for ensuring the time response of the *MR* damping force ( $\sim 40$  ms):

$$\mathcal{F}: \begin{bmatrix} \dot{x}_f \\ u_f \end{bmatrix} = \begin{bmatrix} A_f & B_f \\ C_f \rho_{sat} & 0 \end{bmatrix} \begin{bmatrix} x_f \\ u \end{bmatrix} \quad (6)$$

where,  $\rho_{sat} = \frac{\tanh(C_f x_f / f_0)}{C_f x_f / f_0} \in [0, 1]$  approximates the saturation function of  $u_f$  in:

$$u_{sat} = \begin{cases} f_0 & \text{if } u_f \gg f_0 \\ u_f & \text{if } -f_0 \leq u_f \leq f_0 \\ -f_0 & \text{if } u_f \ll -f_0 \end{cases} \quad (7)$$

Thus, the new structure (8), presented in Figure 2, takes into account the saturation and semi-activity of the damper into the varying parameters.

$$\begin{aligned} \dot{x}_{sf} &= A(\rho_1^*, \rho_2^*) \cdot x_{sf} + B \cdot u + \begin{bmatrix} B_{s1} \\ 0 \end{bmatrix} \cdot z_r \\ y &= [C_s \ 0] \cdot x_{sf} \end{aligned} \quad (8)$$

$$x_{sf} = \begin{bmatrix} x_s \\ x_f \end{bmatrix}, \quad A(\rho_1^*, \rho_2^*) = \begin{bmatrix} A_s + \rho_2^* B_{s2} C_{s2} & \rho_1^* B_s C_f \\ 0_{1 \times 4} & A_f \end{bmatrix}, \quad B = \begin{bmatrix} 0_{4 \times 1} \\ B_f \end{bmatrix}$$

where,  $\rho_1^* = \rho_1 \rho_{sat} \in [-1, 1]$  and  $\rho_2^* = \rho_2 \in [0, 1]$ .

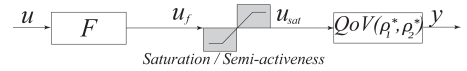


Fig. 2. *QoV* model with a semi-active saturated input.

## 2.3 LPV controller design.

In order to bound the nonlinearities of the closed-loop system, the *LPV* controller computes the manipulation signal by interpolation of a polytope whose vertices are Linear Time-Invariant (*LTI*) controllers. In this case, a polytope of 4 *LTI* controllers is designed by using the  $H_\infty$  control framework; the controller is quadratically stable for all trajectories of the scheduling parameters by solving an optimization problem with *LMI* techniques, Scherer et al. (1997). Figure 3 shows the block diagram for designing the  $H_\infty$  controller in each wheel-station. The weighting functions, based on a priori knowledge of the performance objectives, are designed as:

$$\begin{aligned} W_{z_{r,i}} &= 3 \times 10^{-2}, \quad W_{\ddot{z}_{s,i}} = \frac{K_{s,f} [s^2 + 2\omega_{s1,f} \zeta_{s1,f} s + \omega_{s1,f}^2]}{s^2 + 2\omega_{s2,f} \zeta_{s2,f} s + \omega_{s2,f}^2} \\ W_{z_{us,f}} &= \frac{K_{us,f} [s^2 + 2\omega_{us1,f} \zeta_{us1,f} s + \omega_{us1,f}^2]}{s^2 + 2\omega_{us2,f} \zeta_{us2,f} s + \omega_{us2,f}^2} \\ W_{\ddot{z}_{s,r}} &= \frac{K_{s,r} \omega_{s1,r}^2}{s^2 + 2\omega_{s2,r} \zeta_{s2,r} s + \omega_{s2,r}^2}, \quad W_{z_{us,r}} = \frac{K_{us,r} \omega_{us1,r}}{s + \omega_{us2,r}} \end{aligned}$$

where  $W_{\ddot{z}_{s,i}}$  allows to reduce the amplification of  $\ddot{z}_s$  in each quarter of vehicle for achieving the desired comfort,  $W_{z_{us,i}}$  is shaped to ensure the road holding and  $W_{z_{r,i}}$  increases the sensitivity to the road profile. By considering the control specifications, the generalized model  $\mathcal{P}$  for the *LPV* control synthesis in each wheel-station is,

$$\begin{aligned} \dot{x}_{sf} &= A(\rho_1^*, \rho_2^*) \cdot x_{sf} + B \cdot u + \begin{bmatrix} B_{s1} \\ 0 \end{bmatrix} z_r \\ z &= C_1(\rho_1^*, \rho_2^*) \cdot x_{sf} \cdot \begin{bmatrix} W_{\ddot{z}_{s,i}} & 0 \\ 0 & W_{z_{us,i}} \end{bmatrix} \\ y &= C_2 \cdot x_{sf} \end{aligned} \quad (9)$$

where  $C_1(\rho_1^*, \rho_2^*) = [C_{s1} \ \rho_1^* D_{s1} C_f]$  and,

$$\begin{aligned} C_2 &= [C_{s3} \ 0], \quad C_{s3} = [1 \ 1 \ -1 \ -1], \quad D_{s1} = \begin{bmatrix} -1 \\ m_s \\ 0 \end{bmatrix} \\ C_{s1} &= \begin{bmatrix} -\frac{k_s + b_2}{m_s} & -\frac{b_1}{m_s} & \frac{k_s + b_2}{m_s} & \frac{b_1}{m_s} \end{bmatrix} + \begin{bmatrix} -\frac{f_0}{m_s} \rho_2^* C_{s2} \\ 0_{1 \times 4} \end{bmatrix} \end{aligned}$$

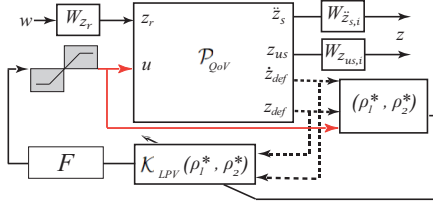


Fig. 3. *LPV* control structure based on  $H_\infty$  framework for an *LTI* model of a *QoV*.

### 3. FEB FORMULATION

The *FEB* controller is considered free of model, only measurements or estimated signals are used to monitor the excitation frequency in the suspension system in order to define the electric current value required to apply over the *MR* damper, and thus achieve the desired control objectives, Lozoya-Santos et al. (2011). This control strategy is considered multi-objective (for comfort and road holding).

Since the frequency of motion in the suspension system ( $f$ ) is an indicator of its performance, with  $f$  it is possible to assign different values of damping coefficient in the semi-active shock absorber according to the frequency responses of the control objectives. Thus, it is possible to hold a specific suspension condition based on an estimated frequency ( $\hat{f}$ ), which is used to manipulate the electric current in bandwidths. The measurements of the deflection velocity ( $\dot{z}_{def} = \dot{z}_s - \dot{z}_{us}$ ) and suspension deflection ( $z_{def} = z_s - z_{us}$ ) are used to estimate the frequency of motion and to decide which damping improves the comfort and/or road holding conditions. By using the *RMS* values of  $z_{def}$  and  $\dot{z}_{def}$  of the *MR* damper piston, the estimation of the frequency in each *QoV* is given by,

$$\hat{f} = \sqrt{\frac{(\dot{z}_{def1}^2 + \dot{z}_{def2}^2 + \dots + \dot{z}_{defn}^2)}{(z_{def1}^2 + z_{def2}^2 + \dots + z_{defn}^2) \cdot 4\pi^2}} \quad (10)$$

where,  $n = 256$  is the number of samples to compute the *RMS* value with a sampling time of  $1/512$ . Since the damping coefficient is proportional to the electric current value in an *MR* damper, a *look-up* table between the manipulation signal (electric current) and the estimated frequency of the suspension motion is defined in order to assure the desired performances for comfort and road holding. Therefore, the *FEB* control law is completely independent of a vehicle or semi-active damper model.

### 4. SIMULATION TESTS

The vehicle model used to evaluate the controllers was characterized from real data (camber angles, caster, damping force, stiffness, etc.) obtained by a *K&C* (Kinematics and Compliance) test over a commercial pickup truck. The model was customized from a generic full-size light-load vehicle model in CarSim<sup>TM</sup> software, Fig. 4, which is used as Software-in-the-Loop (*SiL*). The customization is composed by the physical dimensions (weight, long, width, height, wheel base, front and rear track and so on) and suspension system (independent wheel stations at the front side and a rear solid axle at the back).



Fig. 4. Full-size pickup truck model in CarSim<sup>TM</sup>, by including *MR* dampers in the suspension system.

The Kerb weight is around 2000 Kg, the sprung and unsprung masses as well as the *QoV* model parameters described in eqn. (1) are presented in Table 2.

Table 2. *QoV* model parameters.

| Front <i>QoV</i> |               | Rear <i>QoV</i> |               |
|------------------|---------------|-----------------|---------------|
| Parameter        | Value         | Parameter       | Value         |
| $m_s$            | 630 (Kg)      | $m_s$           | 387 (Kg)      |
| $m_{us}$         | 81.5 (Kg)     | $m_{us}$        | 139.5 (Kg)    |
| $k_s$            | 42,500 (N/m)  | $k_s$           | 37,300 (N/m)  |
| $k_t$            | 295,200 (N/m) | $k_t$           | 295,200 (N/m) |

For *SiL* simulations, the semi-active suspension system is composed by four experimental *MR* damper models described by (2). The characterized *MR* damper is not symmetric in the jounce-rebound effects and only has two levels of actuation: low damping force at 0 A and high damping force at 2.5 A; the range of force is  $[-6000$  to  $11000]$  N (peak to peak), the damper stroke is around 50 mm with a time constant of 12 ms. The model parameters of the shock absorber are shown in Table 3; they were identified from a *chirp* signal with decreasing amplitude from 10 mm to 1 mm at  $[0.5-8]$  Hz. Figure 5 shows the modeling performance of the *Guo* structure.

Table 3. *MR* damper model coefficients.

| Coefficient | Value          | Units |
|-------------|----------------|-------|
| $a_1$       | 21.3843        | s/m   |
| $a_2$       | 14.8223        | 1/m   |
| $b_1$       | 4,630          | s/m   |
| $b_2$       | -3,948.6       | 1/m   |
| $f_c$       | [951.5 - 3067] | N     |

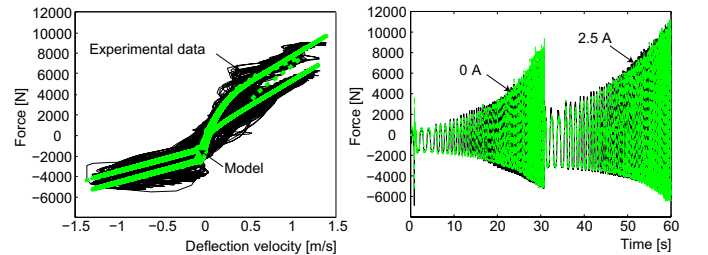


Fig. 5. Comparison between the *MR* damper model and experimental data.

Table 4 shows the parameters of the weighting functions used in the *LPV-H<sub>∞</sub>* control design, the cut frequencies have been selected according to the resonance frequencies of the sprung and unsprung masses, while the damping factors and gains are designed by loop-shaping.

The *BSS* test at 100 Km/h, which explores the most important range of frequencies for comfort and road holding, is used to evaluate the controller performances. The *RMS* value over the variables of interest is used as performance index in order to compare the controller performances respect to the passive one, according to:

$$x = \frac{v_{RMS_{Controller}}}{v_{RMS_{Passive}}} \quad (11)$$



Table 4.  $LPV-H_\infty$  controller parameters.

| Front $QoV$     |          |                  |          |
|-----------------|----------|------------------|----------|
| Parameter       | Value    | Parameter        | Value    |
| $K_{s,f}$       | 1        | $K_{us,f}$       | 10       |
| $\zeta_{s1,f}$  | 0.3      | $\zeta_{us1,f}$  | 0.3      |
| $\omega_{s1,f}$ | 1(rad/s) | $\omega_{us1,f}$ | 9(rad/s) |
| $\zeta_{s2,f}$  | 1        | $\zeta_{us2,f}$  | 1        |
| $\omega_{s2,f}$ | 3(rad/s) | $\omega_{us2,f}$ | 9(rad/s) |
| Rear $QoV$      |          |                  |          |
| Parameter       | Value    | Parameter        | Value    |
| $K_{s,r}$       | 0.1      | $K_{us,r}$       | 0.1      |
| $\omega_{s1,r}$ | 1(rad/s) | $\omega_{us1,r}$ | 9(rad/s) |
| $\zeta_{s2,r}$  | 1        | $\omega_{us2,r}$ | 9(rad/s) |
| $\omega_{s2,r}$ | 3(rad/s) |                  |          |

where  $v$  is the *RMS* value of the variable of interest (pitch, heave and vertical acceleration for comfort, and suspension deflection and tire compression for road holding) during the test,  $RMS_{Controller}$  refers to the controller under analysis and *passive* refers to the baseline suspension system by using a set of passive dampers. When the performance criterion value is greater than the unity, the passive suspension system is better than the semi-active suspension system, i.e. the index  $x$  monitors the improvement or deterioration of the *ASCS*.

## 5. RESULTS AND DISCUSSION

Figure 6 shows the transient response of both controllers respect to the baseline suspension system by considering the *BSS* test. For comfort, the semi-active suspension systems have lower oscillations in the pitch and heave signals close  $t=2$  s (related to 2 Hz), while at  $t>3$  s the vertical acceleration is reduced when the controllers are used. For road holding, the improvement is more significative in whole range of frequencies with both controllers, the damper compression in the front  $QoV$  is reduced up to 20 mm at different time instants (similar results are obtained in the rear damper), while the jounce motion of the rear solid axle is reduced up to 100 mm; by analyzing the tire compression, the improvement is presented between  $t=3$ -5 s, the reduction is up to 10 mm of displacement.

For a quantitative comparison between the *FEB* and *LPV* controllers, Table 5 shows the index of improvement ( $x$ ) obtained by each controller in the *BSS* test. In all variables that monitor the comfort and road holding objectives, both control strategies have better performance than the passive suspension, except the vertical acceleration which in some time instants has lower amplitude in the oscillations caused by the soft suspension.

By comparing the *FEB* and *LPV* transient responses, in almost all variables the *FEB* controller has the best performance. For comfort, the *FEB* controller reduces the pitch angle 19 %; while for road holding, the front suspension deflection is reduced 23% and the rear up to 58%, similarly the tire compression is also reduced up to 10%. On the other hand, Figure 7 shows that the manipulation signal in the *FEB* controller is more persistent with softer changes than the *LPV* controller, whose manipulation depends on the time instant values of the scheduling parameters that could increase the natural waste in the actuation system.

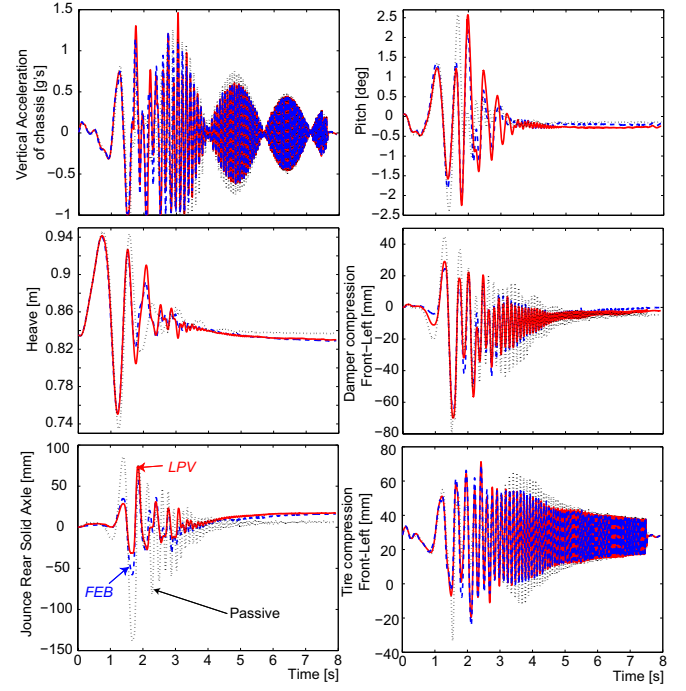


Fig. 6. Performance of the controllers in the *BSS* test.

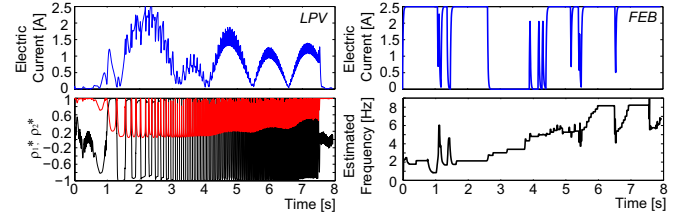


Fig. 7. Control input and control output in both *ASCS*, by analyzing a single wheel station.

## 6. CONCLUSIONS

A comparative analysis between a model-free and a model-based controller is presented in this paper; the full semi-active suspension system considers the four independent wheel stations, each Quarter of Vehicle ( $QoV$ ) has an experimental Magneto-Rheological (*MR*) damper. The Frequency Estimation-Based (*FEB*) controller uses measurements to monitor the frequency of suspension motion in order to apply the required electric current over the *MR* damper; on the other hand, the Linear Parameter-Varying (*LPV*) controller requires a model of the  $QoV$  by including the semi-active damper dynamics. Two measurable scheduling parameters are included in the *LPV* control design to represent the nonlinear behavior (saturation and semi-activeness) of the *MR* damper.

Simulation results of the transient response show that both control strategies improve the comfort and road holding in comparison with the passive suspension system. By comparing the controllers, the *FEB* approach shows slightly the best comfort and road holding performance; the improvement of comfort respect to the passive system includes a reduction of 19% in the pitch angle; while for road holding, the front suspension deflection is reduced 23% and the rear up to 58%, i.e. the lifetime of the dampers is increased. Additionally, *FEB* controller reduces the tire compression up to 10% and *LPV* 17%.

Table 5. Performance comparison respect to the passive suspension system by using the  $x$  index.

| Analysis of comfort      |                                     |                                    |                                   |                                  |                        |
|--------------------------|-------------------------------------|------------------------------------|-----------------------------------|----------------------------------|------------------------|
| Control Approach         | Heave                               | Pitch                              |                                   | Vertical acceleration            |                        |
| <i>FEB</i>               | <b>0.99</b>                         | <b>0.81</b>                        |                                   | <b>1.13</b>                      |                        |
| <i>LPV</i>               | <b>0.99</b>                         | 0.84                               |                                   | 1.14                             |                        |
| Analysis of road holding |                                     |                                    |                                   |                                  |                        |
| Control Approach         | Damper Compression front <i>QoV</i> | Damper Compression rear <i>QoV</i> | Tire Compression front <i>QoV</i> | Tire Compression rear <i>QoV</i> | Jounce rear solid axle |
| <i>FEB</i>               | <b>0.77</b>                         | <b>0.45</b>                        | <b>0.97</b>                       | 0.90                             | <b>0.42</b>            |
| <i>LPV</i>               | 0.84                                | 0.46                               | 0.98                              | <b>0.83</b>                      | 0.46                   |

Finally, the  $LPV-H_\infty$  controller is more complex because requires a reliable model of the whole system, but by design, the asymptotic stability is ensured; on the other hand, the  $FEB$  controller is more feasible to be implemented because only requires process measurements.

## REFERENCES

- Ahmadian, M. (1997). A Hybrid Semiactive Control for Secondary Suspension Applications. In *ASME-ICE, Symp. on Advanced Automotive Tech.*, 743–750. USA.
- Assadsangabi, B., Eghtesad, M., Daneshmand, F., and Vahdati, N. (2009). Hybrid Sliding Mode Control of Semi-Active Suspension Systems. *Smart Materials and Structures*, 18, 1–10.
- Chamseddine, A., Raharijaona, T., and Noura, H. (2006). Sliding Mode Control Applied to Active Suspension using Nonlinear Full Vehicle and Actuator Dynamics. In *IEEE Conf. on Decision and Control*, 3597–3602. USA.
- Do, A., Sename, O., and Dugard, L. (2010). An LPV Control Approach for Semi-Active Suspension Control with Actuator Constraints. In *American Control Conf.*, 4653–4658. USA.
- Dong, X., Yu, M., Li, Z., Liao, C., and Chen, W. (2009). Neural Network Compensation of Semi-active Control for a Magneto-rheological Suspension with Time Delay Uncertainty. *Smart Materials and Structures*, 18, 1–14.
- Dong, X., Yu, M., Liao, C., and Chen, W. (2010). Comparative Research on Semi-Active Control Strategies for Magneto-rheological Suspension. *Nonlinear Dynamics*, 59, 433–453.
- Guo, S., Yang, S., and Pan, C. (2006). Dynamical Modeling of Magneto-rheological Damper Behaviors. *J. of Intell. Mater., Syst. and Struct.*, 17, 3–14.
- Hong, K., Sohn, H., and Hedrick, J. (2002). Modified Skyhook Control of Semi-Active Suspensions: A New Model, Gain Scheduling, and Hardware-in-the-Loop Tuning. *ASME Transactions: J. of Dynamic Systems, Measurement, and Control*, 124, 158–167.
- Hudha, K., Jamaluddin, H., Samin, P., and Rahman, R. (2005). Effects of Control Techniques and Damper Constraint on the Performance of a Semi-Active Magnetorheological Damper. *Int. J. Vehicle Autonomous Systems*, 3, 230–252.
- Ikenaga, S., Lewis, F.L., Campos, J., and Davis, L. (2000). Active Suspension Control of Ground Vehicle Based on a Full-vehicle Model. In *American Control Conf.*, 4019–4024. USA.
- Karnopp, D., Crosby, M., and Harwood, R. (1974). Vibration Control using Semi-active Force Generators. *J. of Eng. for Industry*, 96, 619–626.
- Lozoya-Santos, J., Morales-Menendez, R., Tudón-Martínez, J., Sename, O., Dugard, L., and Ramirez-Mendoza, R. (2011). A LPV Quarter of Car with Semi-active Suspension Model including Dynamic Input Saturation. In *18<sup>th</sup> IFAC World Congress*, 1820–1825. Italy.
- Poussot-Vassal, C., Sename, O., Dugard, L., Gáspár, P., Szabó, Z., and Bokor, J. (2008). A New Semi-active Suspension Control Strategy through LPV Technique. *Control Eng. Practice*, 16, 1519–1534.
- Poussot-Vassal, C., Sename, O., Dugard, L., Gáspár, P., Szabó, Z., and Bokor, J. (2011). Attitude and Handling Improvements Through Gain-scheduled Suspensions and Brakes Control. *Control Eng. Practice*, 19(3), 252–263.
- Sankaranarayanan, V., Emekli, M.E., Güvenç, B.A., Güvenç, L., Öztürk, E.S., Ersolmaz, Ş.S., Eyol, I.E., and Sinal, M. (2008). Semiactive Suspension Control of a Light Commercial Vehicle. *IEEE/ASME Transactions on Mechatronics*, 13(5), 598–604.
- Savaresi, S. and Spelta, C. (2007). Mixed Sky-hook and ADD: Approaching the Filtering Limits of a Semi-active Suspension. *ASME Transactions: J. of Dynamic Systems, Measurement and Control*, 169(4), 382–392.
- Scherer, C., Gahinet, P., and Chilali, M. (1997). Multiobjective Output-feedback Control Via LMI Optimization. *IEEE Transactions on Automatic Control*, 42(7), 896–911.
- Spelta, C., Savaresi, S., and Fabbri, L. (2010). Experimental Analysis of a Motorcycle Semi-active Rear Suspension. *Control Eng. Practice*, 18, 1239–1250.
- Sung, K.G., Han, Y.M., Sohn, J.W., and Choi, S.B. (2008). Road Test Evaluation of Vibration Control Performance of Vehicle Suspension Featuring Electrorheological Shock Absorbers. *J. Automobile Eng.*, 222(5), 685–698.
- Swevers, J., Lauwerys, C., Vandersmissen, B., Maes, M., Reybrouck, K., and Sas, P. (2007). A Model-Free Control Structure for the On-line Tuning of the Semi-Active Suspension of a Passenger Car. *Mechanical Systems and Signal Processing*, 21(3), 1422–1436.
- Tudón-Martínez, J.C., Lozoya-Santos, J., and Morales-Menendez, R. (2012). Efficiency of On-Off Semiactive Suspensions in a Pick-up Truck. *SAE Int. J. Commer. Veh.*, 5(1). Doi:10.4271/2012-01-0979.
- Valasek, M., Novak, M., Sika, Z., and Vaculin, O. (1997). Extended Ground-hook - New Concept of Semi-Active Control of Truck's Suspension. *Vehicle System Dynamics*, 27, 289–303.
- Yoon, J., Cho, W., Kang, J., Koo, B., and Yi, K. (2010). Design and Evaluation of a Unified Chassis Control System for Rollover Prevention and Vehicle Stability Improvement on a Virtual Test Track. *Control Eng. Practice*, 18(6), 585–597.